Robotica (2000) volume 18, pp. 143–151. Printed in the United Kingdom © 2000 Cambridge University Press

Obstacle avoidance control for redundant manipulators using collidability measure

Su Il Choi and Byung Kook Kim

Department of Electrical Engineering, KAIST, 373–1 Kusong-dong, Yusong-gu, Taejon 305–701 (Korea).
E-mail: sichoi@rtel.kaist.ac.kr bkkim@ee.kaist.ac.kr

(Received in Final Form: June 8, 1999)

SUMMARY

We present an efficient obstacle avoidance control algorithm for redundant manipulators using a new measure called *collidability measure*. Considering moving directions of manipulator links, the *collidability measure* is defined as the sum of inverse of predicted collision distances between links and obstacles: This measure is suitable for obstacle avoidance since directions of moving links are as important as distances to obstacles. For kinematic or dynamic redundancy resolution, null space control is utilized to avoid obstacles by minimizing the collidability measure: We present a velocity-bounded *kinematic* control law which allows reasonably large gains to improve the system performance. Also, by clarifying decomposition in the joint acceleration level, we present a simple *dynamic* control law with bounded joint torques which guarantees tracking of a given end-effector trajectory and improves a kinematic cost function such as collidability measure. Simulation results are presented to illustrate the effectiveness of the proposed algorithm.

KEYWORDS: Redundant manipulators; Collidability measure; Velocity-bounded kinematic control; Torque-bounded dynamic control

1. INTRODUCTION

A robot manipulator is defined as *redundant* if it possesses more degrees of freedom than are required to achieve the desired position and orientation of the end-effector. The redundancy of such manipulators can be effectively used to keep within joint limits,[1,2] to avoid singularities,[3] and to optimize various performance criteria.[4–9] Also, we can utilize redundancy to avoid obstacles in workspace.[10–13]

For obstacle avoidance control, many algorithms have been proposed based on pseudoinverse matrix.[10–12] Baillieul[13] proposed the *extended Jacobian technique* for solving the inverse kinematics problem, and applied this technique to obstacle avoidance for a class of planar robots and obstacles. In Khatib's approach,[14] redundant robots are controlled directly in the Cartesian space using a model-based control law, and obstacle avoidance is achieved using an artificial potential field concept. An important feature of this work is the use of simple geometric "primitives" for representing obstacles. However, the selection of representative points on manipulator links is not simple and the distance value doesn't mean the minimum distance between link and obstacle. Rahmanian-Shahri and Troch[15] presented a new method for on-line collision recognition for robot manipulators. For every link and every obstacle in the workspace, a boundary ellipse is defined such that there is no collision if the robot joints are outside these ellipses.

Many of the above mentioned redundancy resolution approaches require a potential function of distances between manipulator and obstacles. Most of the methods assumed that the necessary distance information was given from a higher control level or could be obtained from sensory devices. Gilbert, Johnson, and Keerthi[16] developed an algorithm for computing the Euclidean distance between a pair of convex polytopes. However, the suggested distance algorithm is very complex. In all cases, obstacle avoidance control is acted even when manipulator links move away from obstacles. We are going to remedy this problem by considering moving directions of manipulator links with respect to obstacles.

While many authors have discussed how to specify null-space joint velocities (*kinematic control*), some have considered manipulator dynamics for obstacle avoidance control[11] (*dynamic control*). Ma and Hirose[17] presented an efficient method of including dynamic effects in the obstacle avoidance control of redundant manipulators. This approach is based on a decomposition technique, thus constructing a set of possible solutions for obstacle avoidance. Hsu *et al.*[18] suggested a dynamic control law that guarantees tracking of null-space joint velocities while providing end-effector tracking. Even though the above dynamic control laws are useful, they didn't consider bounds on joint driving torques. Without considering joint torque bounds, excessively large joint torques may be required which is impossible in practice. Hence, efficient kinematic/dynamic control method is necessary considering actuator saturation.

In this paper, we present an efficient obstacle avoidance control algorithm for redundant manipulators using a new measure called *collidability measure*. Considering moving directions of manipulator links, this measure is defined as the sum of inverse of predicted collision distances between links and obstacles. Using the collidability measure, we can reduce the magnitude of obstacle avoidance action considerably, especially when manipulator links move away from obstacles. Also, by clarifying decomposition in the joint acceleration level, we present a simple *dynamic* control law with bounded joint torques which guarantees tracking of a given end-effector trajectory while performing a

https://doi.org/10.1017/S0263574799001861 Published online by Cambridge University Press

subtask such as decreasing collidability measure. In addition, we present velocity-bounded *kinematic* control law which allows reasonably large gain to improve the system performance.

This paper is constructed as follows: In Section 2, the *collidability measure* is defined and derived. In Section 3, velocity-bounded kinematic and torque-bounded dynamic control algorithms are derived for redundancy resolution. Simulation results are presented in Section 4 to illustrate the performance of the proposed algorithm. This paper ends with concluding remarks in Section 5.

2. COLLIDABILITY MEASURE

Consider a redundant manipulator with n degrees of freedom in m dimensional workspace ($n > m$). The forward kinematics and differential kinematics of the manipulator can be represented as

$$\mathbf{x}_e = \mathbf{f}(\boldsymbol{\theta}) \tag{1}$$

$$\dot{\mathbf{x}}_e = J(\boldsymbol{\theta})\dot{\boldsymbol{\theta}} \tag{2}$$

where $\mathbf{x}_e \in R^m$ represents position and orientation of the end-effector, $\boldsymbol{\theta} \in R^n$ represents joint variables, $\mathbf{f}(\boldsymbol{\theta}) \in R^m$ is a vector function describing the manipulator kinematics, and $J(\boldsymbol{\theta}) \in R^{m\times n}$ is the end-effector Jacobian matrix. The general solution of Eq. (2) is

$$\dot{\boldsymbol{\theta}} = J^+\dot{\mathbf{x}}_e + (I - J^+ J)\mathbf{g} \tag{3}$$

where $J^+ = J^T(JJ^T)^{-1}$ is the pseudoinverse of J, $I \in R^{n\times n}$ is the identity matrix, and $\mathbf{g} \in R^n$ is an arbitrary vector in the joint-velocity space which can be used to resolve the redundancy at the velocity level in optimizing a suitable performance criterion.

We use $\mathscr{A}$ and $\mathbb{O}$ to denote the manipulator links and obstacles respectively. The manipulator and obstacles are represented by unions of objects as follows:

$$\mathscr{A} = \bigcup_{i\in I_{\mathscr{A}}} \mathscr{A}_i, \qquad \mathbb{O} = \bigcup_{j\in I_{\mathbb{O}}} \mathbb{O}_j \tag{4}$$

where $\mathscr{A}_i$, $i \in \boldsymbol{I}_{\mathscr{A}} = \{1, \ldots, n\}$ are manipulator links, and $\mathbb{O}_j$, $j \in I_{\mathbb{O}} = \{1, \ldots, n_{\mathbb{O}}\}$ are $n_{\mathbb{O}}$ obstacles. Consider a link-obstacle pair as shown in Figure 1. The problem is to determine a joint trajectory $\boldsymbol{\theta}(t)$ of the manipulator so that its end-effector can move along the desired trajectory while the manipulator A is kept away from obstacles $\mathbb{O}$. Link A_i is assumed to be a cylinder, which can be described as an ellipsoid containing the link cantered at $\mathbf{y}_{ic}$ in the link i coordinate frame described as[19]

$$\mathscr{A}_i(\boldsymbol{\theta}) = \{T_i(\boldsymbol{\theta})\mathbf{y} : (\mathbf{y} - \mathbf{y}_{ic})^T Q_i^T Q_i (\mathbf{y} - \mathbf{y}_{ic}) \le 1\} \tag{5}$$

with

$$Q_i = \begin{bmatrix} 1/r_{ia} & o & 0 \\ 0 & 1/r_{ib} & 0 \\ 0 & 0 & 1/r_{ib} \end{bmatrix} \tag{6}$$

where r_{ia} and r_{ib} are scalar coefficients, and $T_i(\boldsymbol{\theta})$ is a homogeneous transformation matrix for link i coordinate frame which consists of an orthogonal rotation matrix $R_i(\boldsymbol{\theta})$ and a position vector $\mathbf{p}_i(\boldsymbol{\theta})$[20]

$$T_i(\boldsymbol{\theta}) = \begin{bmatrix} R_i(\boldsymbol{\theta}) & \mathbf{p}_i(\boldsymbol{\theta}) \\ 0\ 0\ 0 & 1 \end{bmatrix}. \tag{7}$$

Obstacle $\mathbb{O}_j$ is assumed to be a general convex shape, which can be described as a spherical object containing the obstacle with radius r_j centered at $\mathbf{x}_{jc}$ described as

$$\mathbb{O}_j = \{\mathbf{x} : (\mathbf{x} - \mathbf{x}_{jc})^T S_j^T S_j (\mathbf{x} - \mathbf{x}_{jc}) \le 1\} \tag{8}$$

where

$$S_j = \begin{bmatrix} 1/r_j & 0 & 0 \\ 0 & 1/r_j & 0 \\ 0 & 0 & 1/r_j \end{bmatrix}. \tag{9}$$

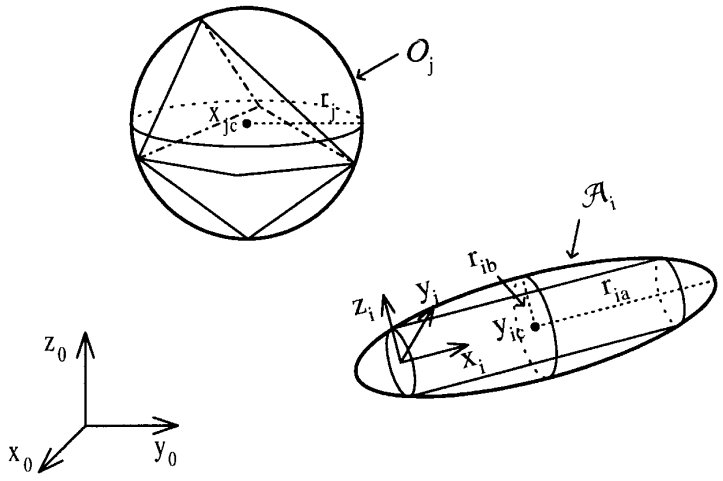

Fig. 1. Link object $\mathscr{A}_i$ and obstacle object ϑ_j.

https://doi.org/10.1017/S0263574799001861 Published online by Cambridge University Press

In order to determine a unique solution of Eq. (3), an additional condition should be introduced, such as minimization of a performance index. Hence, we introduce a new performance measure called *collidability measure* for obstacle avoidance considering moving directions of manipulator links and obstacles, which is defined as the inverse of sum of predicted collision distances between links and obstacles.

Consider now the problem of finding the collidability measure of the link i and the obstacle j. For simplicity of detecting collision between them, elliptical link $\mathcal{A}_i$ and spherical obstacle $\mathcal{O}_j$ are viewed as expanded elliptical link $\hat{\mathcal{A}}_i$ and shrunk point obstacle $\hat{\mathcal{O}}_j$, as shown in Figure 2(a):

$$\hat{\mathcal{A}}_i = \{\mathbf{x} : (\mathbf{x}-\mathbf{x}_{ic})^T Q^T Q(\mathbf{x}-\mathbf{x}_{ic}) \le 1\} \tag{10}$$

$$\hat{\mathcal{O}}_j = \{\mathbf{x} : \mathbf{x} = \mathbf{x}_{jc}\} \tag{11}$$

where $\mathbf{x}_{ic} = T_i(\boldsymbol{\theta})\mathbf{y}_{ic}$, and $Q = (Q_i^{-1} + S_j^{-1})^{-1} R_i^T$. Next, define $\mathbf{x}_c$ as relative position between $\mathbf{x}_{jc}$ and $\mathbf{x}_{ic}$

$$\mathbf{x}_c = \mathbf{x}_{jc} - \mathbf{x}_{ic}. \tag{12}$$

We assume that instantaneous movement of $\mathbf{x}_c$ at time t is maintained during $[t, t+\tau]$ for small τ. Then, the predicted motion of $\mathbf{x}_c$ for primary task (tracking any arbitrary trajectory) is represented as follows:

$$\mathbf{x}_c(t+\tau) = \mathbf{x}_c(t) + \mathbf{v}_c(t)\tau \tag{13}$$

$$\mathbf{v}_c(t) = \dot{\mathbf{x}}_{jc} - \left(\frac{\partial T_i(\boldsymbol{\theta})}{\partial \boldsymbol{\theta}} \dot{\boldsymbol{\theta}}_d(t) \right) \mathbf{y}_{ic} \tag{14}$$

with

$$\dot{\boldsymbol{\theta}}_d(t) = J^+(\boldsymbol{\theta}) \dot{\mathbf{x}}_d(t) \tag{15}$$

where $\mathbf{v}_c(t)$ is the velocity of $\mathbf{x}_c(t)$, $\dot{\boldsymbol{\theta}}_d(t)$ is a desired joint velocity, $\dot{\mathbf{x}}_d(t)$ is a desired end-effector velocity.

Elliptical link $\hat{\mathcal{A}}_i$ will collide with point obstacle $\hat{\mathcal{O}}_j$ if the following conditions are satisfied.

$$\mathbf{v}_c^T Q^T Q \mathbf{x}_c < 0,\ (\mathbf{v}_c^T Q^T Q \mathbf{x}_c)^2 - |Q\mathbf{v}_c|^2 (|Q\mathbf{x}_c|^2 - 1) \ge 0. \tag{16}$$

The predicted collision time t_p is obtained by solving

$$(\mathbf{x}_c + t_p \mathbf{v}_c)^T Q^T Q (\mathbf{x}_c + t_p \mathbf{v}_c) = 1. \tag{17}$$

Then, the predicted collision time t_p and the predicted collision point $\mathbf{x}_p$ are obtained as

$$t_p = \frac{-(\mathbf{v}_c^T Q^T Q \mathbf{x}_c) - \sqrt{(\mathbf{v}_c^T Q^T Q \mathbf{x}_c)^2 - |Q\mathbf{v}_c|^2 (|Q\mathbf{x}_c|^2 - 1)}}{|Q\mathbf{v}_c|^2} \tag{18}$$

$$\mathbf{x}_p = \mathbf{x}_c + t_p \mathbf{v}_c. \tag{19}$$

Using the predicted collision point $\mathbf{x}_p \in \hat{\mathcal{A}}_i$, predicted collision points $\mathbf{x}_{ip} \in \mathcal{A}_i$ and $\mathbf{x}_{jp} \in \mathcal{O}_j$ are obtained as

$$\mathbf{x}_{ip} = \mathbf{x}_{ic} + R_i Q_i^{-1} Q \mathbf{x}_p \tag{20}$$

$$\mathbf{x}_{jp} = \mathbf{x}_{jc} + (R_i Q_i^{-1} Q - I)\mathbf{x}_p \tag{21}$$

Basically, the collidability measure $c_{ij}(\boldsymbol{\theta})$ is defined as the inverse of the predicted collision distance $|\mathbf{x}_{ip} - \mathbf{x}_{jp}|$. In case Eq. (16) is not satisfied, collision will not happen. To make smooth variation of $c_{ij}(\boldsymbol{\theta})$ beyond the collision region, we assume the velocity vector $\mathbf{v}_b$, obtained by rotating $\mathbf{v}_c$ to the origin, makes collision between $\mathcal{O}_j$ and the boundary point of $\hat{\mathcal{A}}_i$. As shown in Figure 2(b), by counterclockwise rotation of $\mathbf{v}_c$ with respect to the vector $\hat{\mathbf{k}}$, $\mathbf{v}_b$ can be obtained as follows:

$$\hat{\mathbf{k}} = \frac{(Q\mathbf{v}_c) \times (-Q\mathbf{x}_c)}{|(Q\mathbf{v}_c) \times (-Q\mathbf{x}_c)|} \tag{22}$$

$$\phi = \cos^{-1}\left(\frac{(Q\mathbf{v}_c) \cdot (-Q\mathbf{x}_c)}{|Q\mathbf{v}_c||Q\mathbf{x}_c|} \right) - \cos^{-1}\left(\frac{\sqrt{|Q\mathbf{x}_c|^2 - 1}}{|Q\mathbf{x}_c|} \right) \tag{23}$$

$$\mathbf{v}_b = Q^{-1} R_{\mathbf{k}}(\phi) Q \mathbf{v}_c \tag{24}$$

where ϕ is the angle difference between $Q\mathbf{v}_c$ and $Q\mathbf{v}_b$, and $R_{\mathbf{k}}(\phi)$ is the rotation matrix. Given the velocity $\mathbf{v}_b$, the boundary collision time t_b and the boundary collision point $\mathbf{x}_b$ on the elliptical link $\hat{\mathcal{A}}_i$ are obtained as

$$t_b = \frac{(Q\mathbf{v}_b) \cdot (-Q\mathbf{x}_c)}{|Q\mathbf{v}_c|^2} = \frac{\sqrt{|Q\mathbf{x}_c|^2 - 1}}{|Q\mathbf{x}_c|} \tag{25}$$

$$\mathbf{x}_b = \mathbf{x}_c + t_b \mathbf{v}_b. \tag{26}$$

Using the boundary collision point $\mathbf{x}_b \in \hat{\mathcal{A}}_i$, boundary collision points $\mathbf{x}_{ib} \in \mathcal{A}_i$ and $\mathbf{x}_{jb} \in \mathcal{O}_j$ are obtained as

$$\mathbf{x}_{ib} = \mathbf{x}_{ic} + R_i Q_i^{-1} Q \mathbf{x}_b \tag{27}$$

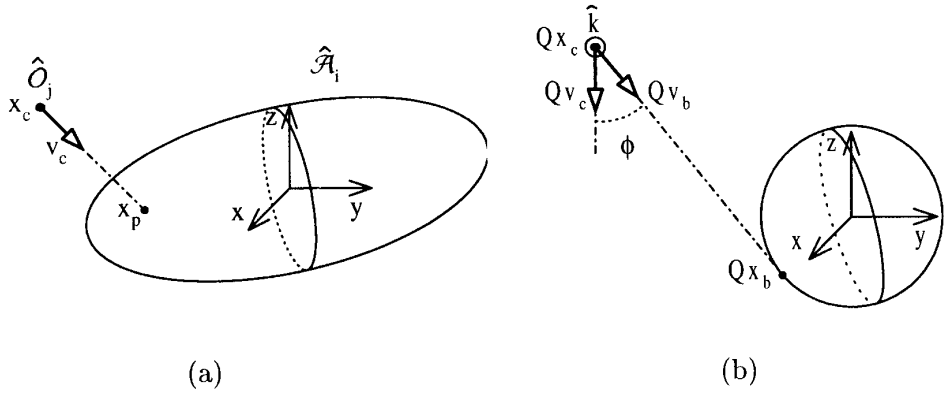

Fig. 2. Collision between $\hat{\mathcal{A}}_i$ and $\hat{\mathcal{O}}_j$: (a) Predicted collision point $\mathbf{x}_p$, (b) Boundary collision point $\mathbf{x}_b$.

https://doi.org/10.1017/S0263574799001861 Published online by Cambridge University Press

$$\mathbf{x}_{jb} = \mathbf{x}_{jc} + (R_i Q_i^{-1} Q - I)\mathbf{x}_b \tag{28}$$

Next, a cubic polynomial of the form

$$g(\phi) = a_0 + a_1\phi + a_2\phi^2 + a_3\phi^3 \tag{29}$$

defined in $0 \le \phi \le \phi_{max}$, where ϕ_{max} represents the angular spline interval, can be splined to fit four boundary conditions of

$$\begin{aligned} g(0) &= \frac{1}{|\mathbf{x}_{ib} - \mathbf{x}_{jb}|} \\ \dot{g}(0) &= \frac{-1}{|\mathbf{x}_{ib} - \mathbf{x}_{jb}|^2} \frac{d|\mathbf{x}_{ib} - \mathbf{x}_{jb}|}{d\phi} \\ g(\phi_{max}) &= 0 \\ \dot{g}(\phi_{max}) &= 0. \end{aligned} \tag{30}$$

The resultant cubic polynomial is

$$g(\phi) = g(0) + \dot{g}(0)\phi - \frac{1}{\phi_{max}^2}(3g(0) + 2\dot{g}(0)\phi_{max})\phi^2 + \frac{1}{\phi_{max}^3}(2g(0) + \dot{g}(0)\phi_{max})\phi^3. \tag{31}$$

Finally, we can get the collidability measure $c_{ij}(\boldsymbol{\theta})$ of the link i and the obstacle j as

$$c_{ij}(\boldsymbol{\theta}) = \begin{cases} \frac{1}{|\mathbf{x}_{ip} - \mathbf{x}_{jp}|} & \text{if Eq. (16) is satisfied} \\ g(\phi) & \text{if } 0 \le \phi \le \phi_{max} \\ 0 & \text{if } \phi > \phi_{max}. \end{cases} \tag{32}$$

The collidability measure between the manipulator and obstacles is obtained as

$$C(\boldsymbol{\theta}) = \sum_{i \in I_{sl},\, J \in I_O} c_{ij}(\boldsymbol{\theta}) \tag{33}$$

Now, we derive $\nabla c_{ij}(\boldsymbol{\theta})$. The continuity and differentiability of $|\mathbf{x}_{ip} - \mathbf{x}_{jp}|$ or $|\mathbf{x}_{ib} - \mathbf{x}_{jb}|$ is necessary to compute $\nabla c_{ij}(\boldsymbol{\theta})$ because $\nabla c_{ij}(\boldsymbol{\theta})$ is dependent on that. The predicted collision distance $|\mathbf{x}_{ip} - \mathbf{x}_{jp}|$ does have a gradient at $\boldsymbol{\theta}$ as

$$\nabla_\theta |\mathbf{x}_{ip} - \mathbf{x}_{jp}| = \nabla_\theta |T_i(\boldsymbol{\theta})\mathbf{y}_{ip} - \mathbf{x}_{jp}| \tag{34}$$

where $\mathbf{y}_{ip} = T_i^{-1}(\boldsymbol{\theta})\mathbf{x}_{ip}$. To be more specific, k-th component of $\nabla|\mathbf{x}_{ip} - \mathbf{x}_{jp}|$ is

$$\begin{aligned} \frac{\partial|\mathbf{x}_{ip} - \mathbf{x}_{jp}|}{\partial\theta_k} &= \frac{(\mathbf{x}_{ip} - \mathbf{x}_{jp})^T}{|\mathbf{x}_{ip} - \mathbf{x}_{jp}|}\left(\frac{\partial T_i(\boldsymbol{\theta})}{\partial\theta_k}\mathbf{y}_{ip}\right) \\ &= \frac{(\mathbf{x}_{ip} - \mathbf{x}_{jp})^T}{|\mathbf{x}_{ip} - \mathbf{x}_{jp}|}[T_{k-1}(\boldsymbol{\theta})\Lambda_k T_{k-1}^{-1}(\boldsymbol{\theta})]\mathbf{x}_{ip} \end{aligned} \tag{35}$$

where ∇_k is a constant matrix.[20] Then, the collidability measure and its partial derivative are obtained as follows:

(a) If the predicted contact point $\mathbf{x}_p$ is obtained:

$$c_{ij}(\boldsymbol{\theta}) = \frac{1}{|\mathbf{x}_{ip} - \mathbf{x}_{jp}|} \tag{36}$$

$$\frac{\partial c_{ij}(\boldsymbol{\theta})}{\partial\theta_k} = \frac{-1}{|\mathbf{x}_{ip} - \mathbf{x}_{jp}|^2}\frac{\partial|\mathbf{x}_{ip} - \mathbf{x}_{jp}|}{\partial\theta_k}. \tag{37}$$

(b) If the boundary contact point $\mathbf{x}_b$ is obtained and $0 \le \phi \le \phi_{max}$:

$$c_{ij}(\boldsymbol{\theta}) = g(\phi) \tag{38}$$

$$\begin{aligned} \frac{\partial c_{ij}(\boldsymbol{\theta})}{\partial\theta_k} &= \frac{\partial g(\phi)}{\partial\phi}\frac{\partial\phi}{\partial\theta_k} \\ &= \frac{\partial g(\phi)}{\partial\phi}\left(\frac{-(Q\mathbf{v}_c)\cdot(Q\frac{\partial\mathbf{x}_{ib}}{\partial\theta_k})}{|Q\mathbf{v}_c||Q(\mathbf{x}_{ib} - \mathbf{x}_{jb})|\sin\phi}\right. \\ &\quad \left. + \frac{\frac{\partial|Q(\mathbf{x}_{ib} - \mathbf{x}_{jb})|}{\partial\theta_k}}{|Q(\mathbf{x}_{ib} - \mathbf{x}_{jb})|\tan\phi}\right). \end{aligned} \tag{39}$$

3. OBSTACLE AVOIDANCE CONTROL

In this section, two redundancy control algorithms—kinematic and dynamic—with actuator constraints are suggested using the collidability measure.

3.1 Velocity-bounded kinematic control

First, a kinematic redundancy control algorithm is developed considering a joint velocity limit, which allows us to use redundant degrees of freedom to perform a subtask while tracking the desired end-effector trajectory.

Let the joint velocity is bounded by

$$|\dot{\boldsymbol{\theta}}_i| \le \dot{\boldsymbol{\theta}}_{i,max}, \quad i \in I_{sl} \tag{40}$$

where $\dot{\boldsymbol{\theta}}_{\mathrm{i,max}}$ is the upper limit of each joint velocity. We can decompose $\dot{\boldsymbol{\theta}}$ in Eq. (3) into range space component $\dot{\boldsymbol{\theta}}_R = J^+\dot{\mathbf{x}}_e$ and null space component $\dot{\boldsymbol{\theta}}_N = (I - J^+J)\mathbf{g}$. For obstacle avoidance, we use the collidability measure $C(\boldsymbol{\theta})$ as an optimization criterion. Then, $\mathbf{g} = \alpha\nabla C$ where ∇C is the gradient of the collidability measure, and α is a gain constant. When $\mathbf{g}$ is large, excessively large null-space joint velocity $\dot{\boldsymbol{\theta}}_N$ is required to achieve the given subtask which violates joint velocity bound. To prevent such a case, we utilize a saturation function, as follows:

Proposition 1: Define a joint velocity saturation function as

$$Sat(\dot{\boldsymbol{\theta}}_N) = \min\left(1, \min_{(\dot{\boldsymbol{\theta}}_N)_i \ne 0,\, i \in I_{sl}} \frac{sgn((\dot{\boldsymbol{\theta}}_N)_i)\dot{\boldsymbol{\theta}}_{i,max} - (\dot{\boldsymbol{\theta}}_R)_i}{(\dot{\boldsymbol{\theta}}_N)_i}\right)\dot{\boldsymbol{\theta}}_N \tag{41}$$

where $(\dot{\boldsymbol{\theta}}_R)_i$ and $(\dot{\boldsymbol{\theta}}_N)_i$ are i-th components of each vector, and $sgn(.)$ is a sign function. Then, each component of the

https://doi.org/10.1017/S0263574799001861 Published online by Cambridge University Press

joint velocity $\dot{\boldsymbol{\theta}} = \dot{\boldsymbol{\theta}}_R + Sat(\dot{\boldsymbol{\theta}}_N)$ satisfies the joint velocity bound $\dot{\boldsymbol{\theta}}_{i,max}$.

Advantages are as follows: This velocity-bounded kinematic control law permits end-effector trajectory tracking while decreasing the possibility of collision via minimizing the collidability measure $C(\boldsymbol{\theta})$. Also, by using $Sat(\dot{\boldsymbol{\theta}}_N)$ instead of $\dot{\boldsymbol{\theta}}_N$, reasonably large α is allowed to improve the system performance.

3.2 Torque-bounded dynamic control

In this subsection, we derive a new dynamic redundancy control algorithm considering joint torque saturation. Differentiating Eq. (2), we obtain the differential relation between the end-effector acceleration and the joint acceleration.

$$\ddot{\mathbf{x}}_e = J\ddot{\boldsymbol{\theta}} + \dot{J}\dot{\boldsymbol{\theta}}. \tag{42}$$

The general solution of Eq. (42) can be obtained using pseudoinverse as

$$\ddot{\boldsymbol{\theta}} = J^+(\ddot{\mathbf{x}}_e - \dot{J}\dot{\boldsymbol{\theta}}) + \ddot{\boldsymbol{\theta}}_N \tag{43}$$

where $\ddot{\boldsymbol{\theta}}_N = (I - J^+J)\mathbf{h}$ is a vector in the null space of J, and $\mathbf{h} \in R^n$ is an arbitrary vector in the joint acceleration space.

Consider the case where the solution of joint velocity is given as Eq. (3) with an arbitrary vector $\mathbf{g} \in R^n$ and we want to obtain the solution of joint acceleration. Differentiating Eq. (3), we obtain the differential Eq. (43) and some relations between them.

Proposition 2: Let's decompose $\ddot{\boldsymbol{\theta}}$ into range space component $\ddot{\boldsymbol{\theta}}_R = J^+(\ddot{\mathbf{x}}_e - \dot{J}\dot{\boldsymbol{\theta}})$ and null space component $\ddot{\boldsymbol{\theta}}_N = (I - J^+J)\mathbf{h}$. Then

$$\ddot{\boldsymbol{\theta}}_R = \left(\frac{d\dot{\boldsymbol{\theta}}_R}{dt}\right)_R + \left(\frac{d\dot{\boldsymbol{\theta}}_N}{dt}\right)_R \tag{44}$$

$$\ddot{\boldsymbol{\theta}}_N = \left(\frac{d\dot{\boldsymbol{\theta}}_R}{dt}\right)_N + \left(\frac{d\dot{\boldsymbol{\theta}}_N}{dt}\right)_N \tag{45}$$

$$\mathbf{h} = \dot{\mathbf{g}} + (J^+\dot{J})^T(\dot{\boldsymbol{\theta}}_R - \mathbf{g}). \tag{46}$$

Proof: Since $\dot{J}^+ = (I - J^+J)\dot{J}^T(JJ^T)^{-1} - J^+\dot{J}J^+$ (see Ma and Hirose[21]), $(J^+)^T = (JJ^T)^{-1}J$, and $JJ^+ = I$, we get

$$\begin{aligned}
\frac{d\dot{\boldsymbol{\theta}}_R}{dt} &= J^+\ddot{\mathbf{x}}_e + \dot{J}^+\dot{\mathbf{x}}_e \\
&= J^+\ddot{\mathbf{x}}_e + \{(I - J^+J)\dot{J}^T(JJ^T)^{-1} - J^+\dot{J}J^+\}\dot{\mathbf{x}}_e \\
&= J^+(\ddot{\mathbf{x}}_e - \dot{J}\dot{\boldsymbol{\theta}}_R) + (I - J^+J)\dot{J}^T(JJ^T)^{-1}\dot{\mathbf{x}}_e \\
&= J^+(\ddot{\mathbf{x}}_e - \dot{J}\dot{\boldsymbol{\theta}}_R) + (I - J^+J)(J^+\dot{J})^T\dot{\boldsymbol{\theta}}_R
\end{aligned} \tag{47}$$

$$\begin{aligned}
\frac{d\dot{\boldsymbol{\theta}}_N}{dt} &= (I - J^+J)\dot{\mathbf{g}} - (\dot{J}^+J + J^+\dot{J})\mathbf{g} \\
&= (I - J^+J)\dot{\mathbf{g}} - \{(I - J^+J)\dot{J}^T(JJ^T)^{-1} \\
&\quad - J^+\dot{J}J^+\}J\mathbf{g} - J^+\dot{J}\mathbf{g} \\
&= (I - J^+J)\{\dot{\mathbf{g}} - \dot{J}^T(JJ^T)^{-1}J\mathbf{g}\} - J^+\dot{J}(I - J^+)\mathbf{g} \\
&= (I - J^+J)\{\dot{\mathbf{g}} - (J^+\dot{J})^T\mathbf{g}\} - J^+\dot{J}\dot{\boldsymbol{\theta}}_N.
\end{aligned} \tag{48}$$

Adding the range-space and null-space terms of Eqs. (47) and (48), respectively, we get

$$\begin{aligned}
\ddot{\boldsymbol{\theta}}_R &= \left(\frac{d\dot{\boldsymbol{\theta}}_R}{dt}\right)_R + \left(\frac{d\dot{\boldsymbol{\theta}}_N}{dt}\right)_R \\
&= J^+(\ddot{\mathbf{x}}_e - \dot{J}\dot{\boldsymbol{\theta}}_R) - J^+\dot{J}\dot{\boldsymbol{\theta}}_N \\
&= J^+(\ddot{\mathbf{x}}_e - \dot{J}\dot{\boldsymbol{\theta}})
\end{aligned} \tag{49}$$

$$\begin{aligned}
\ddot{\boldsymbol{\theta}}_N &= \left(\frac{d\dot{\boldsymbol{\theta}}_R}{dt}\right)_N + \left(\frac{d\dot{\boldsymbol{\theta}}_N}{dt}\right)_N \\
&= (I - J^+J)(J^+\dot{J})^T\dot{\boldsymbol{\theta}}_R + (I - J^+J)\{\dot{\mathbf{g}} - (J^+\dot{J})^T\mathbf{g}\} \\
&= (I - J^+J)\{\dot{\mathbf{g}} + (J^+\dot{J})^T(\dot{\boldsymbol{\theta}}_R - \mathbf{g})\}.
\end{aligned} \tag{50}$$

Adding Eqs. (49) and (50), we get $\ddot{\boldsymbol{\theta}} = \ddot{\boldsymbol{\theta}}_R + \ddot{\boldsymbol{\theta}}_N$ with

$$\mathbf{h} = \dot{\mathbf{g}} + (J^+\dot{J})^T(\dot{\boldsymbol{\theta}}_R - \mathbf{g}). \tag{51}$$

The general form of manipulator dynamics is given by

$$M(\boldsymbol{\theta})\ddot{\boldsymbol{\theta}} + N(\boldsymbol{\theta}, \dot{\boldsymbol{\theta}}) = \boldsymbol{\tau} \tag{52}$$

where $M(\boldsymbol{\theta}) \in R^{n \times n}$ is a symmetric, positive definite inertia matrix, $N(\boldsymbol{\theta}, \dot{\boldsymbol{\theta}}) \in R^n$ is a vector containing nonlinear terms such as Coriolis, centrifugal, and gravitational forces, and $\boldsymbol{\tau} \in R^n$ is a vector of joint actuating torques. Given a desired trajectory, $\mathbf{x}_d(\cdot)$, we want to choose $\boldsymbol{\tau}$ so that the actual trajectory tracks the desired one, as well as achieving a subtask.

A dynamic control law to track a given workspace trajectory is obtained using Eqs. (43) and (52):

$$\boldsymbol{\tau} = M\{J^+(\ddot{\mathbf{x}}_d + K_v\dot{\mathbf{e}} + K_p\mathbf{e} - \dot{J}\dot{\boldsymbol{\theta}}) + \phi_N\} + N \tag{53}$$

where $\mathbf{e} \triangleq \mathbf{x}_d - \mathbf{x}_e$ is the tracking error, K_v and K_p are constant feedback gain matrices, and ϕ_N in any vector in the null space of J. If the manipulator does not go through a singularity, then the control law Eq. (53) guarantees that the tracking error converges to zero.[18]

Next, consider the case where we are given a vector function $\mathbf{g} = \alpha\nabla C(\boldsymbol{\theta}) \in R^n$ for obstacle avoidance and we want the null space joint velocity to track the projection of $\mathbf{g}$ onto the null space of J, where α is a gain constant. Since $(I - J^+J)$ projects vectors onto the null space of J, this is the same as asking that

$$\dot{\mathbf{e}}_N \triangleq (I - J^+J)\mathbf{g} - \dot{\boldsymbol{\theta}}_N \tag{54}$$

converge to zero. The following proposition shows how to choose ϕ_N to get the desired result.

Proposition 3: Assume that the manipulator does not go through a singularity. Let the control be given by Eq. (53) with

$$\phi_N = (I - J^+J)\{\dot{\mathbf{g}} + (J^+\dot{J})^T(\dot{\boldsymbol{\theta}}_R - \mathbf{g}) + K_N\dot{\mathbf{e}}_N\} \tag{55}$$

where K_N is a positive definite feedback matrix. Then the tracking error $\mathbf{e}$ converges to zero and the joint velocity converges to $\mathbf{g}$ in the null space of J, i.e., $\dot{\mathbf{e}}_N \rightarrow 0$.

https://doi.org/10.1017/S0263574799001861 Published online by Cambridge University Press

Proof: Differentiating Eq. (54), we get $\frac{d\dot{\mathbf{e}}_N}{dt}$ as

$$\begin{aligned}\frac{d\dot{\mathbf{e}}_N}{dt} &= (I-J^+J)\dot{\mathbf{g}} - (\dot{J}^+J + J^+\dot{J})\mathbf{g} \\ &\quad - \left\{\left(\frac{d\dot{\boldsymbol{\theta}}_N}{dt}\right)_R + \left(\frac{d\dot{\boldsymbol{\theta}}_N}{dt}\right)_N\right\} \\ &= (I-J^+J)\{\dot{\mathbf{g}} - (J^+\dot{J})^T\mathbf{g}\} - J^+\dot{J}(I-J^+J)\mathbf{g} \\ &\quad - \left\{\ddot{\boldsymbol{\theta}}_N + \left(\frac{d\dot{\boldsymbol{\theta}}_N}{dt}\right)_R - \left(\frac{d\dot{\boldsymbol{\theta}}_R}{dt}\right)_N\right\} \\ &= (I-J^+J)\{\dot{\mathbf{g}} + J^+\dot{J})^T(\dot{\boldsymbol{\theta}}_R - \mathbf{g})\} - \ddot{\boldsymbol{\theta}}_N \\ &\quad - J^+\dot{J}\{(I-J^+J)\mathbf{g} - \dot{\boldsymbol{\theta}}_N\} \end{aligned} \tag{56}$$

since $\dot{J}^+J + J^+\dot{J} = (I-J^+J)(J^+\dot{J})^T + J^+J(I-J^+J)$. Substituting for $\ddot{\boldsymbol{\theta}}_N$ from Eqs. (53) and (55), we get

$$\begin{aligned}\frac{d\dot{\mathbf{e}}_N}{dt} &= (I-J^+J)\{\dot{\mathbf{g}} + (J^+\dot{J})^T(\dot{\boldsymbol{\theta}}_R - \mathbf{g})\} - \phi_N - J^+\dot{J}\dot{\mathbf{e}}_N \\ &= -(I-J^+J)K_N\dot{\mathbf{e}}_N - J^+\dot{J}\dot{\mathbf{e}}_N \end{aligned} \tag{57}$$

since $\ddot{\boldsymbol{\theta}}_N = (I-J^+J)\ddot{\boldsymbol{\theta}}$ and ϕ_N belongs to the null space of J.

Define a Lyapunov function $v()$ by

$$v = \frac{1}{2}\|\dot{\mathbf{e}}_N\|^2. \tag{58}$$

Then, $\dot{v}$ becomes

$$\begin{aligned}\dot{v} &= \dot{\mathbf{e}}_N^T\frac{d\dot{\mathbf{e}}_N}{dt} \\ &= -\dot{\mathbf{e}}_N^T(I-J^+J)K_N\dot{\mathbf{e}}_N - \dot{\mathbf{e}}_N^TJ^+\dot{J}\dot{\mathbf{e}}_N \\ &= -\dot{\mathbf{e}}_N^TK_N\dot{\mathbf{e}}_N \end{aligned} \tag{59}$$

since $(I-J^+J)^T = (I-J^+J)$, $(I-J^+J)(I-J^+J) = (I-J^+J)$, and $(I-J^+J)J^+ = 0$. Since v is positive definite and $\dot{v}$ is negative definite, $\|\dot{\mathbf{e}}_N\|$ goes to zero monotonically. □

Additionally, we can also obtain the same result from the dynamic control law, which is proposed by Hsu *et al.*[18] as follows:

$$\begin{aligned}\boldsymbol{\phi}_N &= (I-J^+J)(\dot{\mathbf{g}} + K_N\dot{\mathbf{e}}_N) - (J^+\dot{J}J^+ + \dot{J}^+)J(\mathbf{g} - \dot{\boldsymbol{\theta}}) \\ &= (I-J^+J)(\dot{\mathbf{g}} + K_N\dot{\mathbf{e}}_N) \\ &\quad - (I-J^+J)\dot{J}^T(JJ^T)^{-1}J(\mathbf{g} - \dot{\boldsymbol{\theta}}) \\ &= (I-J^+J)\{\dot{\mathbf{g}} + (J^+\dot{J})^T(\dot{\boldsymbol{\theta}} - \mathbf{g}) + K_N\dot{\mathbf{e}}_N\} \\ &= (I-J^+J)\{\dot{\mathbf{g}} + (J^+\dot{J})^T(\dot{\boldsymbol{\theta}}_R - \mathbf{g}) + K_N\dot{\mathbf{e}}_N\} \end{aligned} \tag{60}$$

since $(J^+\dot{J})^T\dot{\boldsymbol{\theta}} = (J^+\dot{J})^T\dot{\boldsymbol{\theta}}_R$. Our dynamic control law is much simpler than that of Hsu *et al.*[18] because our method doesn't need to compute $\dot{J}^+$.

Let the joint torque is bounded by

$$|\boldsymbol{\tau}_i| \le \boldsymbol{\tau}_{i,max}, \qquad i \in \boldsymbol{I}_{\mathcal{A}} \tag{61}$$

where $\boldsymbol{\tau}_{\mathrm{i,max}}$ is the upper limit of each joint torque. Decompose $\boldsymbol{\tau}$ as $\boldsymbol{\tau} = \boldsymbol{\tau}_R + \boldsymbol{\tau}_N$ where

$$\begin{aligned}\tau_R &= MJ^+(\ddot{\mathbf{x}}_d + K_v\dot{\mathbf{e}} + K_p\mathbf{e} - \dot{J}\dot{\boldsymbol{\theta}}) + N \\ \tau_N &= M\phi_N \end{aligned} \tag{62}$$

In some cases, excessively large null space joint torque $\boldsymbol{\tau}_N$ is required to achieve the given subtask. To prevent such a case, we utilize a saturation function as follows.

Proposition 4: Define a torque saturation function as

$$Sat(\boldsymbol{\tau}_N) = \min\left(1, \min_{(\boldsymbol{\tau}_N)i \neq 0, i=1,\cdots,n} \frac{sgn((\boldsymbol{\tau}_N)_i)\boldsymbol{\tau}_{i,max} - (\boldsymbol{\tau}_R)_i}{(\boldsymbol{\tau}_N)_i}\right)\boldsymbol{\tau}_N \tag{63}$$

Then, each component of the joint torque $\boldsymbol{\tau} = \boldsymbol{\tau}_R + Sat(\boldsymbol{\tau}_N)$ satisfies the torque bound $\boldsymbol{\tau}_{i,max}$.

The function $(I-J^+J)\mathbf{g}$ can be thought of as the desired null space joint velocity, where $\mathbf{g} = \alpha\nabla C$. Hence, the purpose of this dynamic control law is to make the self-motion or the null space joint velocity $\dot{\boldsymbol{\theta}}_N = (I-J^+J)\dot{\boldsymbol{\theta}}$ track the projection of $\mathbf{g}$ on the null space of J, which is the same as asking that $\dot{\mathbf{e}}_N$ should converge to zero. This dynamic control law permits end-effector trajectory tracking while decreasing

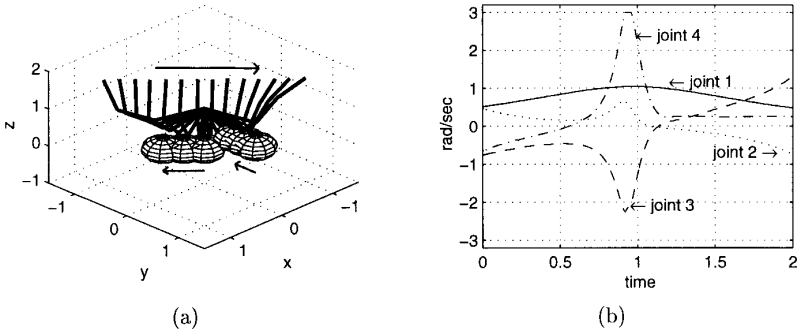

(a) (b)

Fig. 3. Kinematic obstacle avoidance control with collidability measure: (a) Trajectories, (b) Joint velocities.

https://doi.org/10.1017/S0263574799001861 Published online by Cambridge University Press

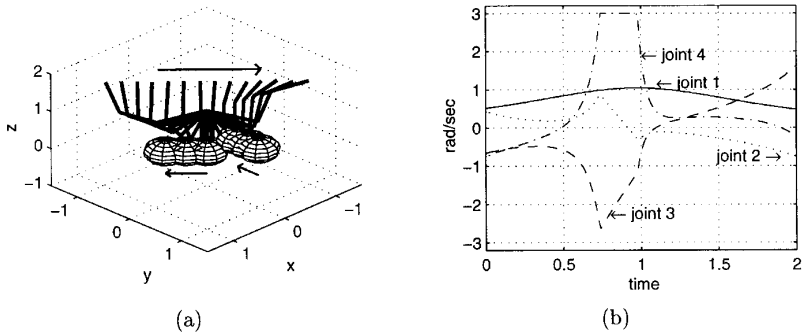

Fig. 4. Kinematic obstacle avoidance control with conventional measure: (a) Trajectories, (b) Joint velocities.

the possibility of collision via minimizing the collidability measure.

Major advantages of the torque-bounded dynamic control law are as follows. Utilizing the decomposed $\ddot{\boldsymbol{\theta}}$ in Proposition 2, our dynamic control law is much simpler than that of Hsu *et al.*[18] Also, by using $Sat(\boldsymbol{\tau}_N)$ instead of $\boldsymbol{\tau}_N$, reasonably large α is allowed to improve the system performance.

4. SIMULATION

Consider a four-link manipulator moving in three dimensional space with two spherical obstacles. We choose parameters as follows: Link lengths ($l_i = 1$ *m*, $i = 1, \cdots, 4$), link masses ($m_i = 10$ *kg*, $i = 1, \cdots, 4$), inertia parameters ($I_i = 5/6\ kgm^2$, $i = 1, \cdots, 4$).

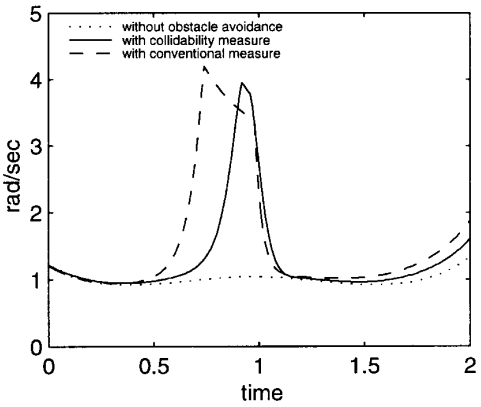

Fig. 5. Joint velocity norm for three cases.

First, the kinematic obstacle avoidance control is simulated with the desired trajectory, which is given as a straight line Cartesian path with a constant velocity $\dot{\mathbf{x}}_d = [-1\ 1\ 0]^T$ *m/sec* for $t_f = 2.0$ seconds. We choose $\mathbf{g} = \alpha_1 \nabla C + \alpha_2 \nabla H$ to minimize the collidibility measure $C(\boldsymbol{\theta})$ and maximize the manipulability measure $H(\boldsymbol{\theta}) = \sqrt{det(JJ^T)}$, where $\alpha_1 = -0.4$ and $\alpha_2 = 0.1$ are gain constants. Two spherical obstacles do uniform motion, and the joint velocity bound $\dot{\boldsymbol{\theta}}_{i,max} = 3$ *rad/sec*, $i = 1, \cdots, 4$. Using kinematic control algorithm with the collidibility measure, Figure 3(a) shows the resultant trajectory with moving obstacles. Joint velocities are shown in Figure 3(b).

For comparison, kinematic obstacle avoidance control with a conventional measure – inverse of minimum distance – is simulated. In this case, Figure 4(a) shows the resultant trajectory with moving obstacles. Joint velocities are shown in Figure 4(b). Comparing Figure 3(b) and Figure 4(b), the collidability measure produces much less joint motions or null-space joint motions than that of the conventional measure. Hence, the joint velocity norm of the collidability measure is reduced, which is shown in Figure 5 when compared with the conventional measure, because relative movements of manipulator links and obstacles are considered.

Next, the dynamic obstacle avoidance control is simulated. The desired trajectory is given as a straight line Cartesian path starting and ending with zero velocity, with constant bang-bang type acceleration/deceleration $\ddot{\mathbf{x}}_d = [-1\ 1\ 0]^T\ m/sec^2$. We use the same kinematic criteria

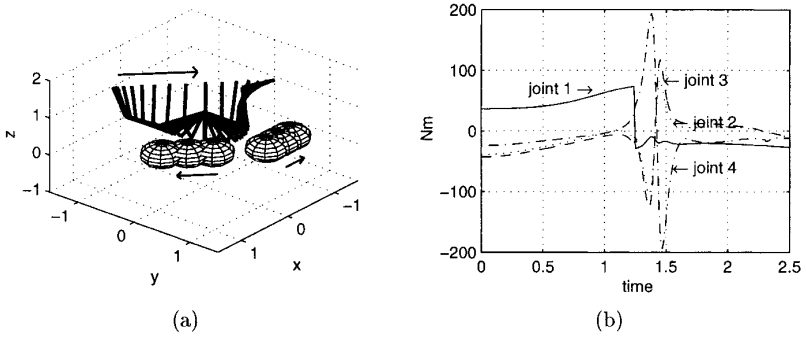

Fig. 6. Dynamic obstacle avoidance control with collidability measure: (a) Trajectories, (b) Joint torques.

https://doi.org/10.1017/S0263574799001861 Published online by Cambridge University Press

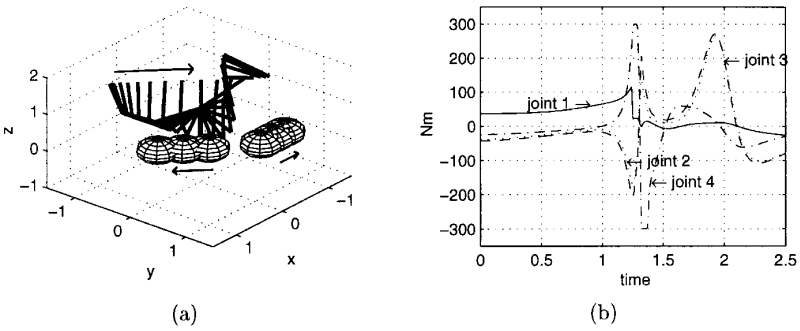

(a) (b)

Fig. 7. Dynamic obstacle avoidance control with conventional measure: (a) Trajectories, (b) Joint torques.

as in the case of kinematic control except $\alpha_1 = -0.292$ and $\alpha_2 = 0.1$, and $\boldsymbol{\tau}_{i,max} = 300\ Nm$, $i = 1, \cdots, 4$. In the case of dynamic obstacle avoidance control with the collidability measure, the resultant trajectory with moving obstacles is shown in Figure 6(a). In addition, Figure 6(b) shows joint torques for the collidability measure.

In the case of dynamic obstacle avoidance control with the conventional measure, Figure 7(a) shows the resultant trajectory with moving obstacles. Joint torques for the conventional measure are shown in Figure 7(b). Comparing Figure 6(a) and Figure 7(a), the amount of variation of configuration (or joint velocity) for obstacle avoidance with the collidability measure is much less than that with the conventional measure. This is because relative movements of manipulator links and obstacles are considered for obstacle avoidance. Also, joint torques in Figure 8 shows that obstacle avoidance control with the collidability measure is economic, since it requires much less joint torque than the conventional measure.

Various simulations are performed to reveal that our control algorithm with the collidability measure satisfies joint velocity or torque bound, and requires less null space control action for obstacle avoidance, leaving more actions possible for improving other measures such as manipulability measure.

5. CONCLUSION

We presented a new measure called *collidability measure* for obstacle avoidance control of redundant manipulators.

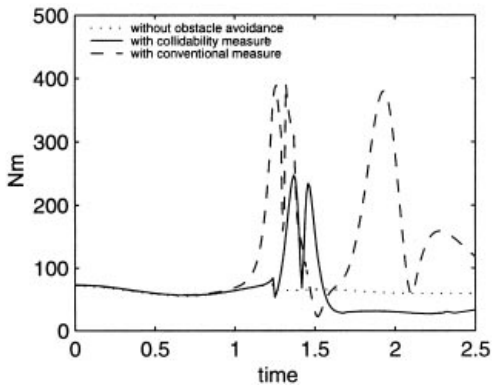

Fig. 8. Joint torque norm for three cases.

Obstacle avoidance action is reduced remarkably, since the collidability measure is obtained based on the relative movements of manipulator links and obstacles, and produces less null space control action. We also clarified decomposition into range and null spaces in the joint velocity/acceleration level, and presented velocity-bounded kinematic control law and simple dynamic control law with bounded joint torque which guarantee asymptotic tracking of a desired trajectory while performing desired subtasks. These control laws satisfy joint velocity or torque bound, and allow a reasonable large gain constant to improve the system performance. Effectiveness of our control laws have been demonstrated with various simulations.

References

1. A. Liegeois, "Automatic supervisory control of the configuration and behavior of multi-body mechanisms," *IEEE Trans. on Ssytem, Man, and Cybernetics* **7**, No. 12, 868–871 (1977).
2. C.A. Klein and C. Huang, "Review of pseudoinverse control for use with kinematically redundant manipulators," *IEEE Trans. on Ssytem, Man, and Cybernetics* **13**, No. 3, 245–250 (1983).
3. T. Yoshikawa, "Manipulability of robot mechanism," *Int. J. Robitics Research* **4**, No. 2, 3–9 (1985).
4. O. Khatib, "Dynamic control of manipulator in operational space," *Proc. 6th IFFToMM World Congress on Theory of Machines and Mechanisms* (1983) pp. 1128–1131.
5. J. Baillieul, J.M. Hollerbach and R. Brochett, "Programming and control of kinematically redundant manipulators," *Proc. 23rd Conf. on Decision and Control* (1984) pp. 768–774.
6. J.M. Hollerbach and K.C. Suh, "Redundancy resolution of manipulators through torque optimization," *Proc. IEEE Int. Conf. on Robotics and Automation* (1985), pp. 1016–1021.
7. J.M. Hollerbach and K.C. Suh, "Redundancy resolution of manipulators through torque optimization," *IEEE J. Robotics and Automation* **3**, No. 4, 308–315 (1987).
8. S. Hirose and S. Ma, "Redundancy decomposition control for multi-joint manipulators," *Proc. IEEE Int. Conf. on Robotics and Automation* (1989) pp. 119–124.
9. S. Ma, D. Nenchev and S. Hirose, "Improving local torque optimization techniques for redundant robotic mechanisms," *Int. J. Robotic Systems* **8**, No. 1, 75–91 (1991).
10. A.A. Maciejewski and C.A. Klein, "Obstacle avoidance for kinematically redundant manipulators in dynamically varying environments," *Int. J. Robotics Research* **4**, No. 3, 109–117 (1985).
11. Y. Nakamura, H. Hanafusa and T. Yoshikawa, "Task-priority based on redundant control of robot manipulators," *Int. J. Robotics Research* **6**, No. 2, 3–15 (1987).
12. M. Kircanski and M. Vukobratovic, "Contribution to control

https://doi.org/10.1017/S0263574799001861 Published online by Cambridge University Press

of redundant robotic manipulators in an environment with obstacles," *Int. J. Robotics Research* **5**, No. 4, 112–119 (1986).
13. J. Baillieul, "Avoiding obstacles and resolving kinematic redundancy," *IEEE Int. Conf. on Robotics and Automation* (1986), pp. 1698–1704.
14. O. Khatib, "Real-time obstacle avoidance for manipulators and mobile robots," *Int. J. Robotics Research* **5**, No. 1, 90–98 (1986).
15. N. Rahmanian-Shari and I. Troch, "Collision-avoidance control for redundant articulated robots," *Robotica* **13**, Part, 2, 159–168 (1995).
16. E.G. Gilbert, D.W. Johnson, and S.S. Keerthi, "A fast procedure for computing the distance between complex objects in three-dimensional space," *IEEE J. Robotics and Automation* **4**, No. 2, 193–203 (1988).
17. S. Ma and S. Hirose, "A dynamic approach to real-time obstacle avoidance control of redundant manipulators," *JSME Int. J.*, series C, **39**, No. 2, 317–322 (1996).
18. P. Hsu, J. Hauser and S. Sastry, "Dynamic control of redundant manipulators," *J. Robotic Systems* **6**, No. 2, 133–148 (1989).
19. C.J. Wu, "On the representation and collision detection of robots," *J. Intelligent and Robotic Systems* **16**, 151–168 (1996).
20. K.S. Foo, R.C. Gonzalez, and C.S.G. Lee, *Robotics: Control, Sensing, Vision and Intelligence* (McGraw-Hill, New York, 1987).
21. S. Ma and S. Hirose, "Dynamic redundancy resolution of redundant manipulators with local optimization of a kinematic criterion," *Proc. 2nd Asian Conf. of Robotics and its Application* (1994), pp. 236–243.

https://doi.org/10.1017/S0263574799001861 Published online by Cambridge University Press